Available online at www.sciencedirect.com
SCIENCE DIRECT®
Journal of Sound and Vibration 276 (2004) 381–400
JOURNAL OF SOUND AND VIBRATION
www.elsevier.com/locate/jsvi

Dynamic stability analysis of non-linear structures with geometrical imperfections under random loading

T. Most[a,*], C. Bucher[a], Y. Schorling[b]

[a] *Institute of Structural Mechanics, Bauhaus-Universität Weimar, Marienstrasse 15, D-99423 Weimar, Germany*
[b] *HOCHTIEF, Frankfurt a.M., Germany*

Received 17 June 2002; accepted 22 July 2003

Dedicated to Professor Y.K. Lin (Florida Atlantic University) on the occasion of his 80th birthday

Abstract

This article presents selected research results in the field of stochastic dynamic stability problems. Both the geometrical properties and the loading conditions are supposed to be random in nature. The stability behavior of structures excited by time-dependent loads can be described by the maximum Lyapunov exponent. This exponent turns positive for unstable systems and can be computed by a non-linear time integration with simultaneous stability analysis. Alternatively, an approximation can be obtained by investigating a linearized version of the structural model. The non-linear time integration of large structures requires a huge numerical effort, thus this method is limited by available computer capacities. In this article both methods are applied and the respective results are compared for geometrically perfect and imperfect systems of different sizes.

1. Introduction

This document gives a survey of several investigations in stochastic dynamic stability analysis. In previous publications the authors considered geometrically imperfect structures with static loading [1] and periodic loading conditions [2,3] by using stability analysis of the linearized system. The non-linear equation of motion of the system was linearized and the Lyapunov exponents for almost sure stability were computed by using the FLOQUET theory [4]. This linearization was based on an expansion of the stiffness matrix of the system into an asymptotic series with respect to a static loading parameter.

*Corresponding author.
E-mail address: thomas.most@bauing.uni-weimar.de (T. Most).

0022-460X/$ - see front matter © 2003 Elsevier Ltd. All rights reserved.
doi:10.1016/j.jsv.2003.07.038

In Ref. [2], Itô analysis [5] was applied for cases of random loading. Stability was expressed in terms of the long-term behavior of the second moments. The main difficulty in this investigation was to analyze the effect of random imperfections. These geometrical imperfections are interpreted as randomly spatially distributed deviations from a perfect geometry. Mathematically, they are represented by random fields discretized at points which are equivalent to the nodes of the finite element model. The covariance matrix of such a random field can be diagonalized [6] by means of a similarity transformation based on the eigenvectors of the covariance matrix. These eigenvectors can be interpreted as spatially orthogonal imperfection shapes with probabilistic weights. The influence of these imperfection shapes on the stability behavior can be analyzed separately for each shape using standard methods of structural mechanics.

A quite complete review of bifurcations of non-linear systems is given by To and Li [7]. Here analytical expressions for the largest Lyapunov exponent are derived using an amplitude–phase transformation. This is extremely useful for single degree-of-freedom systems (s.d.o.f.). Unfortunately, it is not a simple task to expand their approach to cover arbitrary multiple degree-of-freedom systems (m.d.o.f.). Consequently, numerical procedure are required as e.g., proposed by To and Liu [8]. This paper actually refers to an earlier publication by Wolf et al. [9].

A later publication of Schorling et al. [10] investigated non-linear systems under random loading. The approach presented there is based on the convergence criterion "stability with probability one" (almost sure stability). The stability of the structure is determined by analyzing the tangential equations of motion of the structure as obtained from a consistent linearization, see, e.g., Refs. [4,11,12]. This procedure theoretically requires a time integration of the system with an accompanying stability analysis until infinity. For this analysis type arbitrary non-linearities of the system can be considered, however, at the price of generating the system matrices at each time step. Obviously for this method the time integration of the system is the crucial numerical operation. The random loading is described by a scalar-valued random process. It is assumed to be stationary in time and normally distributed with a given mean value and power spectral density. By using a finite Fourier series representation with random coefficients [13] the process can be discretized within a given frequency band.

In this article the stability analysis based on non-linear time integration is explained. Systems with different types and sizes are investigated. Problems in the application of the method as outlined are exemplified. Finally, the reliability analysis of a non-linear shell structure with geometrical imperfection modelled by random fields is presented in detail. All analysis tasks are performed with the SLang Software package [14,15].

2. Stability concept

2.1. Basics

Stability analysis investigates the long-term behavior of motion under the influence of perturbations [4,16]. For a stable motion, perturbations are insignificant, the perturbed motion stays close to the unperturbed motion. In the unstable case an infinitesimal perturbation causes a considerable change of the motion. Depending on the type of perturbation, the stability analysis is sub-classified in structural stability and stability in Lyapunov sense. The structural stability

analysis investigates the effect of perturbed system properties such as mass, stiffness and damping [17,18]. The stability concept in Lyapunov sense analyses the effect of perturbations of the initial conditions.

An unperturbed motion x_1 is called stable in the Lyapunov sense if for any given $\varepsilon > 0$ there is a $\delta(\varepsilon) > 0$ so that for any perturbed motion $x_2(t)$ with

$$\|x_1(t_0) - x_2(t_0)\| < \delta, \tag{1}$$

one has

$$\|x_1(t) - x_2(t)\| < \varepsilon, \tag{2}$$

for all $t, t_0 \in \mathbb{R}^+$ [4]. In Fig. 1 both solutions are displayed.

A motion satisfying Eq. (2) is asymptotically stable if the condition

$$\lim_{t \to \infty} \|x_1(t) - x_2(t)\| = 0, \tag{3}$$

is fulfilled. For the stability analysis it is useful to investigate the behavior of the perturbed neighboring motion $x_2(t)$. It is only necessary to describe the long-term behavior of

$$y(t) = x_2(t) - x_1(t). \tag{4}$$

The asymptotic stability condition Eq. (3) gets the form

$$\lim_{t \to \infty} \|y(t)\| = 0. \tag{5}$$

2.2. Application in structural dynamics

The equation of motion of non-linear dynamic systems is usually given in the form

$$\mathbf{M}\ddot{\mathbf{x}} + \mathbf{r}(\mathbf{x}, \dot{\mathbf{x}}) = \mathbf{f}, \tag{6}$$

where $\mathbf{M}$ is the mass matrix, $\mathbf{x}$ the displacement vector, $\mathbf{r}$ the non-linear restoring force vector and $\mathbf{f}$ a time depending continuous loading function. The dimension of this system of equations is N. The linearization of Eq. (6) leads to

$$\mathbf{r} = \mathbf{r}(\mathbf{x}_0, \dot{\mathbf{x}}_0) + \mathbf{C}\dot{\mathbf{y}} + \mathbf{K}\mathbf{y}, \tag{7}$$

with $\mathbf{y} = \mathbf{x} - \mathbf{x}_0$ as the deviation from the reference solution and $\mathbf{K}$ and $\mathbf{C}$ as the tangential stiffness and damping matrices [10]. The equation of motion may be split in a differential equation

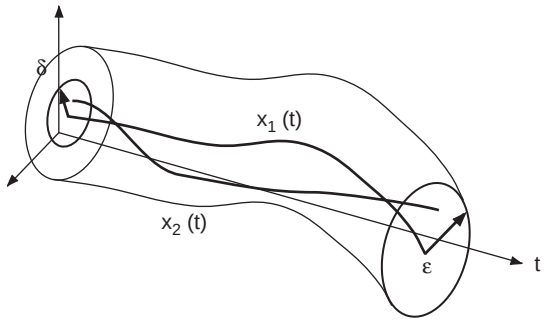

Fig. 1. Stability in Lyapunov sense.

for the reference solution itself,

$$\mathbf{M}\ddot{\mathbf{x}}_0 + \mathbf{r}(\mathbf{x}_0, \dot{\mathbf{x}}_0) = \mathbf{f}, \tag{8}$$

and a differential equation for the neighboring (tangential) motions

$$\mathbf{M}\ddot{\mathbf{y}} + \mathbf{C}\dot{\mathbf{y}} + \mathbf{K}\mathbf{y} = \mathbf{0}. \tag{9}$$

To apply the Lyapunov stability analysis a transformation into the state space $\mathbf{z}^{\mathrm{T}} = (\mathbf{y}^{\mathrm{T}}, \dot{\mathbf{y}}^{\mathrm{T}})$ is helpful:

$$\dot{\mathbf{z}} = \begin{bmatrix} \mathbf{0} & \mathbf{I} \\ \mathbf{M}^{-1}\mathbf{K} & \mathbf{M}^{-1}\mathbf{C} \end{bmatrix} \mathbf{z}, \tag{10}$$

or abbreviated

$$\dot{\mathbf{z}} = \mathbf{A}[\mathbf{x}_0(t)]\mathbf{z}. \tag{11}$$

The Lyapunov exponents are a measure for the average exponential divergence or convergence of neighboring orbits in the phase space. They represent universal stability properties of arbitrary dynamical processes. The kth one-dimensional Lyapunov exponent is defined [19] by

$$\lambda_{ik} = \lim_{t\to\infty} \frac{1}{t} \ln \|\mathbf{z}_k(t)\| / \|\mathbf{z}_k(t_0)\|, \quad k \in [1, 2N]. \tag{12}$$

$\mathbf{z}_k$ denotes a set of linearly independent perturbation vectors in the phase space. For a linear system with constant coefficients, the λ_k correspond to the real parts of the eigenvalues. The largest Lyapunov exponent decides upon stability of the process [20]

$$\left.\begin{array}{ll} \text{stable} & \text{if} \quad \max \lambda_k < 0, \\ \text{unstable} & \text{if} \quad \max \lambda_k > 0, \end{array}\right\}, \quad k = 1, \ldots, 2N. \tag{13}$$

The states of $\mathbf{z}(t_n)$, $t_n = t_0 + n\Delta t$ can be determined with the fundamental matrix $\mathbf{\Theta}$

$$\mathbf{z}(t_n) = \mathbf{\Theta}(t_n, t_{n-1})\mathbf{z}(t_{n-1}). \tag{14}$$

In case the time interval $\Delta t = t_n - t_{n-1}$ is chosen small enough to consider the term $\mathbf{A}(t)$ constant within any interval, the transition matrix between the time steps may be derived analytically (e.g., Ref. [21]) as

$$\mathbf{\Theta}(t_n, t_{n-1}) = \mathbf{R}(t_{n-1}) \operatorname{diag}(\mathrm{e}^{\kappa_i \Delta t}) \mathbf{R}(t_{n-1})^{-1}. \tag{15}$$

The transition matrix from time 0 to t is then approximated by the product

$$\mathbf{\Theta}(t, 0) = \prod_{n=1,\mathrm{nstep}} \mathbf{\Theta}(t_n, t_{n-1}). \tag{16}$$

The Lyapunov exponents can be determined by solving the eigenvalue problem

$$\mathbf{\Theta}(t, t_0)\mathbf{z} = \mu\mathbf{z}, \tag{17}$$

with this equation [19]

$$\tilde{\lambda}_k = \lim_{t\to\infty} \frac{1}{t - t_0} \ln|\mu_k|. \tag{18}$$

Here the tilde indicates the approximation to Eq. (12) introduced by the time discretization in Eq. (14). The presented procedure requires the exact determination of the tangential matrices (consistent linearization) and it easily enables the detection of the complete Lyapunov exponent spectrum.

2.3. Stochastic stability

The elements of the system matrix **A** in Eq. (11) are random processes in the case of stochastic excitation. This implies that stability can only be checked in terms of probabilities or expected values. Based on the asymptotic stability condition of the state-space vector

$$\lim_{t\to\infty} ||\mathbf{z}|| = 0, \tag{19}$$

different stability conditions may be defined [22,23]:

Stability with probability one or almost sure or sample stability

$$P\left[\lim_{t\to\infty} ||\mathbf{z}|| = 0\right] = 1. \tag{20}$$

Stability in probability

$$P\left[\lim_{t\to\infty} ||\mathbf{z}|| > \varepsilon\right] = 0 \quad \forall \varepsilon > 0. \tag{21}$$

Stability in mean square or stability in second moments

$$\lim_{t\to\infty} E[||\mathbf{z}||^2] = 0. \tag{22}$$

The most stringent criterion of these is given by the stability in mean square.

The top Lyapunov exponent for almost sure stability $\tilde{\lambda}_{\max}$ can be determined by a limiting process

$$\tilde{\lambda}_{\max}(\mathbf{x}_0, \mathbf{s}) = \lim_{t\to\infty} \frac{1}{t} \log ||\boldsymbol{\Theta}(\mathbf{x}_0, t)\mathbf{s}||, \tag{23}$$

in which **s** is an arbitrary unit vector. Based on the multiplicative ergodic theorem (e.g., Ref. [24]) the Lyapunov exponent can also be calculated as an expected value

$$\tilde{\lambda}_{\max}(\mathbf{x}_0, \mathbf{s}) = E\left[\frac{\mathrm{d}}{\mathrm{d}t} \log ||\boldsymbol{\Theta}(\mathbf{x}_0, t)\mathbf{s}||\right]. \tag{24}$$

The norm $||\boldsymbol{\Theta}(\mathbf{x}_0, t)\mathbf{s}||$ can be expressed in terms of

$$||\boldsymbol{\Theta}(\mathbf{x}_0, t)\mathbf{s}|| \leqslant ||\boldsymbol{\Theta}(\mathbf{x}_0, t)|| \cdot ||\mathbf{s}|| = ||\boldsymbol{\Theta}(\mathbf{x}_0, t)||. \tag{25}$$

In this equation, a matrix norm must be chosen which is compatible to the vector norm used in Eq. (23). If the Euclidean vector norm is used, equality in Eq. (25) is obtained by choosing the matrix norm equal to the eigenvalue $\mu_{\max}$ of $\boldsymbol{\Theta}(\mathbf{x}_0, t)$ with maximum absolute value (cf. Eq. (18)).

This result is used in calculating the Lyapunov exponent according to Eq. (23). The limit for t has to be taken at some finite value for which convergence can be assumed. For the statistical estimation of the convergence of the Lyapunov exponent, Eq. (24) is suitable.

3. Structural analysis

3.1. Modal reduction and time integration

In order to reduce the system size a modal reduction can be applied, in which the equation of motion Eq. (42) is projected into a subspace defined by m modes of vibration Φ_i of the structure which correspond to the lowest natural frequencies. These mode shapes are the solutions to

$$(\mathbf{K}(\mathbf{x}_{\text{stat}}) - \omega_i^2 \mathbf{M})\boldsymbol{\Phi} = \mathbf{0}, \quad i = 1, \ldots, m, \tag{26}$$

in which $\mathbf{x}_{\text{stat}}$ is a reference solution, typically chosen to be the static solution under permanent loading. To obtain real eigenvalues, which are necessary for the modal reduction, the reference solution $\mathbf{x}_{\text{stat}}$ has to be chosen in that way, that stable modes of vibration exist. The mode shapes obtained with Eq. (26) are assumed to be mass normalized:

$$\boldsymbol{\Phi}^{\mathrm{T}} \mathbf{K}(\mathbf{x}_{\text{stat}})\boldsymbol{\Phi} = \operatorname{diag}(\omega_i^2), \tag{27}$$

with

$$\boldsymbol{\Phi}^{\mathrm{T}} \mathbf{M} \boldsymbol{\Phi} = \mathbf{I}. \tag{28}$$

By assuming modal damping the linear damping matrix $\mathbf{C}$ can be obtained from the eigenvalues ω_i and the modal damping ratios D_i in the form

$$\mathbf{C} = \boldsymbol{\Phi}^{-\mathrm{T}} \operatorname{diag}(2D_i\omega_i)\boldsymbol{\Phi}^{\mathrm{T}}. \tag{29}$$

A transformation $\mathbf{y} = \boldsymbol{\Phi}\mathbf{v}$ and a multiplication of Eq. (6) with $\boldsymbol{\Phi}^{\mathrm{T}}$ represents a projection of the differential equation of motion into the subspace of dimension m as spanned by the eigenvectors obtained from solving Eq. (26)

$$\ddot{\mathbf{v}} + \boldsymbol{\Phi}^{\mathrm{T}} \mathbf{r}(\mathbf{x}, \dot{\mathbf{x}}) = \boldsymbol{\Phi}^{\mathrm{T}} \mathbf{f}. \tag{30}$$

The integration of this equation by the central difference method [25] requires a time step less than $\Delta t_{\text{crit}} = 2\omega_m^{-1}$ (approximation for a linear system). This is considerably large than the critical time step for the full system (Eq. (6)). The time integration in the subspace and the computation of the restoring forces on the full system causes the following problem: If the initial displacement or velocity vector of the time integration is not zero, for example due to static loading, the projection of these vectors into the subspace leads to an optimization problem caused by the higher number of variables in the full space. By using a least-squares approach

$$\mathbf{v} = \boldsymbol{\Phi}^{-1}\mathbf{x}; \quad \boldsymbol{\Phi}^{-1} = (\boldsymbol{\Phi}^{\mathrm{T}}\boldsymbol{\Phi})\boldsymbol{\Phi}^{\mathrm{T}}, \tag{31}$$

this projection is optimally approximated, but not suitable for a subspace spanned by a small number of eigenvectors. A possibility for handling this, is to start the time integration in the subspace with a displacement and velocity vector equal to zero. The initial vectors have to be saved in the full system and the restoring force vector has to be computed by addition of the initial and the time integration vectors

$$\mathbf{r}(\mathbf{x}, \dot{\mathbf{x}}) = \mathbf{r}(\mathbf{x}_{\text{init}} + \boldsymbol{\Phi}\mathbf{v}, \dot{\mathbf{x}}_{\text{init}} + \boldsymbol{\Phi}\dot{\mathbf{v}}), \qquad \mathbf{v}(t=0) = \dot{\mathbf{v}}(t=0) = \mathbf{0}. \tag{32}$$

The stability of the reference solution $\mathbf{x}_0(t)$ is determined by the long-term behavior of the neighboring motion (Eq. (9)). For m.d.o.f. systems this equation could be projected into the same

subspace as in Eq. (30)

$$\ddot{\mathbf{w}} + \mathbf{\Phi}^{\mathrm{T}}\mathbf{C}\mathbf{\Phi}\dot{\mathbf{w}} + \mathbf{\Phi}^{\mathrm{T}}\mathbf{K}\mathbf{\Phi}\mathbf{w} = \mathbf{0}. \tag{33}$$

The subspace of the neighboring motion could also be smaller than of the reference solution, because a smaller number of modes is necessary to approximate the stability behavior then to map the motion of the system.

Even for the commonly employed Rayleigh or the somewhat more general modal damping assumption Eq. (29) remains a system of coupled equations, as the term $\mathbf{K}$—which depends on the reference solution—is not diagonalized by the matrix of eigenvectors. Eq. (33) may be transformed into its state-space description as defined by $\mathbf{z}^{\mathrm{T}} = (\mathbf{w}^{\mathrm{T}}, \dot{\mathbf{w}}^{\mathrm{T}})$ as

$$\dot{\mathbf{z}} = \begin{bmatrix} \mathbf{0} & \mathbf{I} \\ -\mathbf{\Phi}^{\mathrm{T}}\mathbf{K}\mathbf{\Phi} & -\mathbf{\Phi}^{\mathrm{T}}\mathbf{C}\mathbf{\Phi} \end{bmatrix} \mathbf{z}. \tag{34}$$

3.2. Random excitation

The time-dependant loading function is assumed to be of the form

$$\mathbf{f} = \mathbf{f}_0 + v(t)\mathbf{f}_{\mathrm{fluct}}, \tag{35}$$

where $v(t)$ is a scalar *white noise* random process with zero mean value and the power spectral density $S_{vv}(\omega)$. The *white noise* process is characterized by a infinitely wide frequency band. To compute discrete samples of the random process it is necessary to fix the maximum and the decomposition of this frequency band. In this form, $v(t)$ is represented by Fourier series (using FFT)

$$v_r(t) = \sum_{s=1}^{r} \sigma_s(A_s \cos \omega_s t + B_s \sin \omega_s t). \tag{36}$$

The Fourier coefficients A_s, B_s are zero-mean Gaussian random variables with unit standard deviation. The random amplitudes are given as [13]

$$\sigma_s^2 = \int_{\Delta\omega_s} S_{vv}(\omega)\,\mathrm{d}\omega \approx S_{vv}(\omega_s)\Delta\omega_s. \tag{37}$$

In this case the spectrum is not smooth caused by the random amplitudes. To obtain a smooth spectrum, the amplitudes have to be deterministic values. Then the Fourier coefficients and the amplitudes are given as [26]

$$A_s = B_s = 1, \qquad \sigma_s^2 \approx S_{vv}\Delta\omega_s, \qquad S_{vv} = S_{vv}(\omega_1) = \cdots = S_{vv}(\omega_r). \tag{38}$$

3.3. Random imperfections

Geometrical imperfections are interpreted as spatially fluctuating structural properties with respect to a perfect geometry. They are modelled as random fields, described by a mean and covariance function and a defined degree of homogeneity and isotropy [27]. For simplicity the random imperfections considered in this article are assumed to be weakly homogeneous and

normally distributed. An exponential correlation function with a defined correlation length l_h is used.

If the random field is discretized at the nodes of a finite element structure the correlation matrix may be determined in a straightforward manner as a function of the nodal co-ordinates [28]. Support conditions of the structure have considerable influence on the stability behavior. In order to isolate such effects the location of the supports is assumed to be deterministic, while the structure itself remains geometrically imperfect. Mathematically, this step is carried out by conditioning the random field. The resulting *conditional* random field [27,29] then has vanishing variances at the supports and non-vanishing variances in the remaining structure and thus is no longer weakly homogeneous. Its parameters are determined via a stochastic interpolation scheme which is based on the maximum likelihood principle [29].

The correlation matrix $\hat{\mathbf{C}}_{xx}$ finally obtained is diagonalized:

$$\mathbf{\Psi}^{\mathrm{T}}\hat{\mathbf{C}}_{xx}\mathbf{\Psi} = \mathrm{diag}(\sigma^2_{Y_j}) \quad \text{with } \sigma^2_{Y_1} \geqslant \sigma^2_{Y_2} \geqslant \cdots \sigma^2_{Y_p}, \tag{39}$$

where p is the total number of random variables of the random field. The eigenvectors $\mathbf{\Psi}$ can be interpreted as imperfections shapes, the eigenvalues $\sigma^2_{Y_j}$ represent variances of the respective amplitudes. In this representation these amplitudes are normally distributed, have zero mean and for convenience are ordered with decreasing size [28].

The failure probability of the structure is computed by integration of the marginal distribution of the random variable vector $\mathbf{Y}$ over the failure domain indicated by $g(\mathbf{y}) \leqslant 0$

$$p_f = \int_{g(\mathbf{y})<0} f_{\mathbf{Y}}(\mathbf{y})\,\mathrm{d}\mathbf{y}. \tag{40}$$

In the case of failure due to loss of stability, $g(\mathbf{y}) \leqslant 0$ corresponds to the case $\tilde{\lambda}_{\max} > 0$. To solve Eq. (40) imperfection shapes are increased until the stability border is reached. When $f_{\mathbf{Y}}$ is of dimension one the failure probability may be calculated analytically. An interaction model between the random variables can be applied for higher dimensions. A procedure like the response surface method [28] combined with adaptive sampling strategies [30] gives accurate results for the solution of Eq. (40) as long as the dimension of the random variable vector $f_{\mathbf{Y}}$ remains sufficiently small. This requires a sensitivity study to identify the most important random variables.

The stability behavior for the different imperfection shapes may be analyzed for non-linear and linearized systems.

3.4. Linearization

In order to analyze non-linear systems by methods of linear dynamics, the non-linear system matrices have to be linearized. Usually, the non-linear stiffness matrix in Eq. (9) is approximated by an asymptotic series with respect to the load $\varphi v(t)$:

$$\mathbf{K} = \mathbf{K}(\mathbf{x}_{\mathrm{stat}}) + \varphi v(t)\mathbf{K}_1 + \varphi^2 v^2(t)\mathbf{K}_2 + \cdots. \tag{41}$$

In this equation, $\mathbf{x}_{\mathrm{stat}}$ is chosen to be the displacement solution of Eq. (8) under static loading. The matrices $\mathbf{K}_i$ and the factor φ may be determined by static equilibrium conditions. First-order approximation of Eq. (41) by assuming smallness of $\varphi v(t)$ leads to the following linearized

differential equation of the neighboring motions

$$\mathbf{M}\ddot{\mathbf{y}} + \mathbf{C}\dot{\mathbf{y}} + (\mathbf{K}(\mathbf{x}_{\text{stat}}) + \varphi v(t)\mathbf{K}_1)\mathbf{y} = \mathbf{0}. \tag{42}$$

Applying modal reduction (Eqs. (30)–(42)) and transforming the result into its state-space description as defined by $\mathbf{z}^{\mathrm{T}} = (\mathbf{v}^{\mathrm{T}}, \dot{\mathbf{v}}^{\mathrm{T}})$ according to Eq. (10) leads to

$$\dot{\mathbf{z}} = \begin{bmatrix} \mathbf{0} & \mathbf{I} \\ -\text{diag}(\omega_i^2) & -\text{diag}(2D_i\omega_i) \end{bmatrix}\mathbf{z} + \begin{bmatrix} \mathbf{0} & \mathbf{0} \\ -\mathbf{\Phi}^{\mathrm{T}}\mathbf{K}_1\mathbf{\Phi} & \mathbf{0} \end{bmatrix}\mathbf{z}\varphi v(t), \tag{43}$$

or abbreviated,

$$\dot{\mathbf{z}} = \mathbf{A}(t)\mathbf{z}, \quad \mathbf{A}(t) = \mathscr{A} + \mathscr{B}\varphi v(t), \tag{44}$$

with the constant coefficient matrices $\mathscr{A}$ and $\mathscr{B}$.

4. Numerical examples

4.1. Convergence properties

The s.d.o.f. system in Eq. (45) was investigated with the sample analysis.

$$m\ddot{x} + c\dot{x} + k[1 + \ell v(t)]x = 0. \tag{45}$$

In this example the excitation $v(t)$ is assumed to be a broadband random process with zero mean and unit standard deviation. Time series for this process are calculated by using Eq. (36). This means that a number of periodic functions with different frequencies are added. The phase angles are random quantities. The load factor ℓ is increased from 0.5 to 2.0 in four steps. Fig. 2 shows the time-dependent mean value and standard deviation of the estimated Lyapunov exponents for the third load level obtained from 50 simulations, each having 35000 time steps at $\Delta t = \pi \times 10^{-2}$ s. The figure clearly indicates that the estimate for the Lyapunov exponent is a random quantity. This is a consequence of the band limitation ($\omega_{\max}$) and the spectral discretization ($\Delta\omega$) of the white noise. It can be observed that both the mean value $\bar{\lambda}_{\max}$ and the standard deviation $\sigma_{\tilde{\lambda}_{\max}}$ are quite stable after a certain number of time steps. Fig. 3 shows three samples obtained by using 100000 time steps with the same step size as above, where different limit values are obtained. Therefore the average of many simulations is necessary to obtain a fast convergence of the mean value.

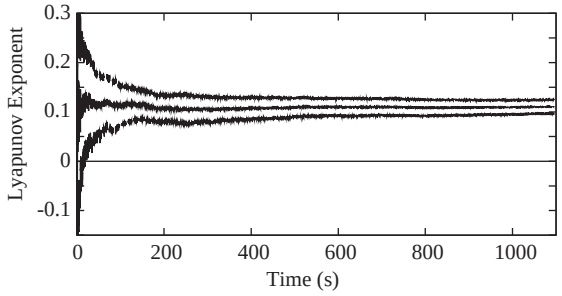

Fig. 2. Top Lyapunov exponent for s.d.o.f.-system for load factor 1.5.

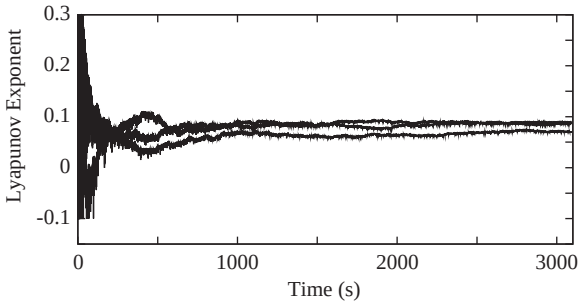

Fig. 3. Top Lyapunov exponent for s.d.o.f.-system for different samples.

Table 1
Top Lyapunov exponents obtained by sample analysis and Lin/Cai approach

ℓ	Sample analysis	Lin/Cai
0.25	-0.0939 ± 0.0013	-0.093864
0.50	-0.0758 ± 0.0019	-0.075456
0.75	-0.0453 ± 0.0040	-0.044777
1.00	-0.0031 ± 0.0051	-0.001825
1.25	0.0517 ± 0.0059	0.053398
1.50	0.1155 ± 0.0095	0.120893
1.75	0.1890 ± 0.0143	0.200660

The Lyapunov exponent of linear s.d.o.f. systems under white noise excitation can be approximated analytically according to Lin and Cai [23]:

$$\hat{\lambda}_{\max} = -D\omega_0 + \pi S_{vv}\omega_0^2/4, \tag{46}$$

in which $\omega_0 = \sqrt{k/m}$, D is modal damping ratio and S_{vv} is the power spectral density of the white-noise excitation. An improved approximation can be obtained using the approach by Pardoux and Wihstutz [31] which takes the series expansion of the Lyapunov exponent in terms of the noise intensity up to second order terms. In the present example this proved not to be necessary.

Eq. (46) was applied to the s.d.o.f. given in Eq. (45). The excitation power spectral density has to be obtained from the power spectral density of the unit random process and the load factor as

$$S_{vv,\mathrm{exc}} = \ell^2 S_{vv,f(t)}. \tag{47}$$

The random process spectral density $S_{ff,f(t)}$ can be calculated from the band limitation of the two-sided frequency band by the relation

$$S_{vv,f(t)} = 1/2\omega_{\max} = \Delta t/2\pi. \tag{48}$$

The obtained analytical Lyapunov exponents are shown in Table 1 in comparison to numerical results from the sample analysis obtained by calculating 50 simulations with 10^5 time steps. The agreement is excellent.

4.2. Analytical solution and verification

A direct analytical solution of the differential equation system like Eq. (45) in terms of elementary integrations is possible if the system matrix $\mathbf{A}(t)$ can be transformed to a triangular matrix by a time-independent transformation $\mathbf{T}$. This is practicable e.g., if $\mathbf{A}(t)$ has identical column-sums

$$\mathbf{A}(t) = \begin{bmatrix} 0 & 1 \\ -1 & -2 \end{bmatrix} + \begin{bmatrix} 0 & 0 \\ -1 & -1 \end{bmatrix} \ell v(t). \tag{49}$$

The transformation takes place as follows

$$\dot{\mathbf{v}} = \mathbf{T}^{-1}\mathbf{A}(t)\mathbf{T}\mathbf{v} \quad \text{with } \dot{\mathbf{z}} = \mathbf{A}(t)\mathbf{z}, \ \ \mathbf{z} = \mathbf{T}\mathbf{v}. \tag{50}$$

The transformation matrix is given as

$$\mathbf{T}(t) = \begin{bmatrix} 1 & 0 \\ -1 & 1 \end{bmatrix}, \quad \mathbf{T}^{-1} = \begin{bmatrix} 1 & 0 \\ 1 & 1 \end{bmatrix}, \tag{51}$$

and leads to the differential equation system

$$\begin{bmatrix} \dot{v}_1 \\ \dot{v}_2 \end{bmatrix} = \begin{bmatrix} -1 & 1 \\ 0 & -1 - \ell v(t) \end{bmatrix} \begin{bmatrix} v_1 \\ v_2 \end{bmatrix}. \tag{52}$$

As solutions of this equations

$$v_1 = v_{1,0} \mathrm{e}^{-t} \mathrm{e}^{\int_0^t \ell v(\tau)\,\mathrm{d}\tau}, \quad v_2 = v_{2,0} \mathrm{e}^{-t} \int_0^t \mathrm{e}^{\int_0^\tau \ell v(\zeta)\,\mathrm{d}\zeta}\,\mathrm{d}\tau + v_{1,0}\mathrm{e}^{-t}. \tag{53}$$

The obtained transformed monodromy matrix

$$\mathbf{\Theta}^*(t,0) = \mathrm{e}^{-t} \begin{bmatrix} 1 & \int_0^t \mathrm{e}^{\int_0^\tau \ell v(\zeta)\,\mathrm{d}\zeta}\,\mathrm{d}\tau \\ 0 & \mathrm{e}^{\int_0^t \ell v(\tau)\,\mathrm{d}\tau} \end{bmatrix}, \quad \mathbf{v}(t) = \mathbf{\Theta}^*(t,0)\mathbf{v}(0) \tag{54}$$

can be transformed back. The eigenvalues of the solved monodromy matrix lead to the top Lyapunov exponent:

$$\kappa_{\mathbf{\Theta},1} = \mathrm{e}^{-t}, \quad \kappa_{\mathbf{\Theta},2} = \mathrm{e}^{-t}\mathrm{e}^{\int_0^t \ell v(\tau)\,\mathrm{d}\tau},$$

$$\lambda_1^*(t) = -1, \quad \lambda_2^*(t) = -1 - \frac{1}{t}\int_0^t \ell v(\tau)\,\mathrm{d}\tau,$$

$$\lambda_{\max}(t) = \max(\lambda_1^*(t), \lambda_2^*(t)). \tag{55}$$

For the comparison of the analytical and the numerical Lyapunov exponents it is necessary to solve the time integral of the excitation process. For a discretized white-noise process this is only possible by numerical integration. For random excitation the Lyapunov exponents were calculated and verified for a unstable load level. The relative deviations between the numerical and the analytical solutions did not exceed a value of 2.5×10^{-6} as displayed in Fig. 4.

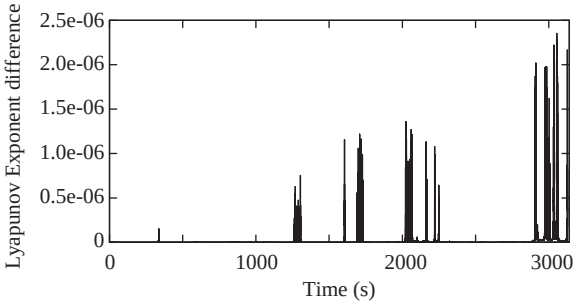

Fig. 4. Relative deviation of the numerical maximum Lyapunov exponent from the analytical solution for random excitation.

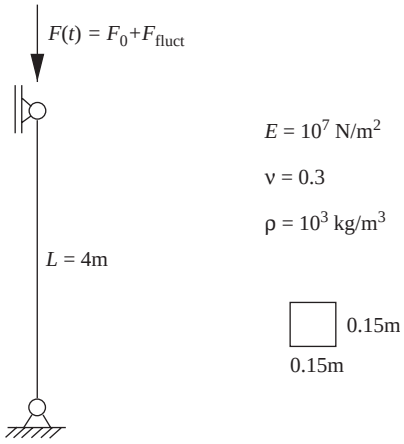

Fig. 5. m.d.o.f.-Column subjected to parametric excitation.

4.3. *Effect of modal reduction on non-linear analysis*

To analyze the non-linear stability behavior of m.d.o.f. systems, the above mentioned explicit time integration procedure is applied. It is then necessary to compute the tangential stiffness matrix at every time step. This necessitates the reduction into a smaller subspace in order to reduce the huge numerical effort. The size of this subspace has to be large enough to reproduce the dynamic behavior adequately. This can be checked by comparing simulations of the full and the reduced system.

The simple column as shown in Fig. 5 is analyzed with the non-linear sample analysis. The system is modelled with 20 geometrically non-linear beam elements with 60 d.o.f. by enabling only displacements in one plane. The static load F_0 is chosen to be 80% of the critical load of the perfect column. A non-linear static stability analysis leads to the value of $F_{\text{crit}} = 259.2$ N. The dynamic load is chosen to be a Gaussian white noise. For the dynamic stability analysis, a modal damping ratio of $D_k = 0.01$ is assumed for all modes.

To check how many modes are necessary to reproduce the dynamic behavior of the full system, different modal subspaces were investigated. Fig. 6 compares the Lyapunov exponents obtained from analyses with $m = 20$ and 60 modes, respectively. The latter case corresponds to a full

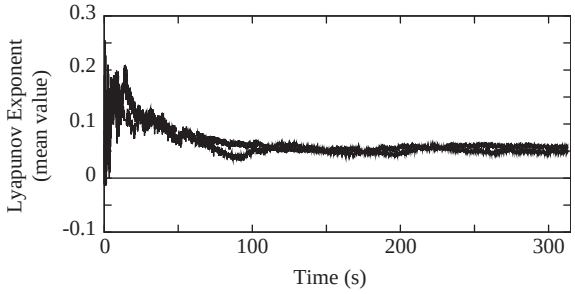

Fig. 6. Influence of modal reduction on the top Lyapunov exponent.

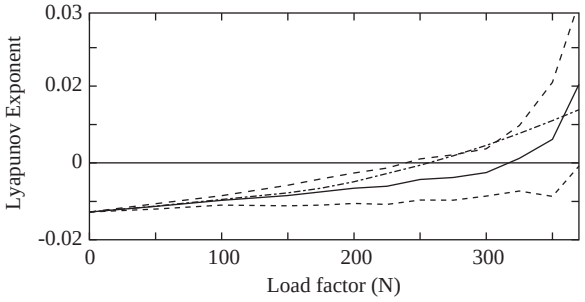

Fig. 7. Comparison of top Lyapunov exponents from the analysis of the non-linear and linearized system: —, mean value; - - - -, standard deviation; -·-·-·-, linear.

explicit analysis. Critical time steps were one order of magnitude apart so that $m = 20$ led to a speed-up of 10. The time steps for this simulation were assumed with $\Delta t = \pi \times 10^{-4}$ s for the full system and $\Delta t = \pi \times 10^{-3}$ s for the reduced system. The used load factor of 400 N leads to an unstable motion. Due to the smaller time step it has to be multiplied the with factor $\sqrt{10}$ for the full system to get the same intensity value of the white noise.

By using this size of the subspace for the time integration and the respective time step, the Lyapunov exponents for different load levels were computed by calculating 100 simulation with 10^5 time steps each. The stability analysis itself does not need a large number of modes, it is important that the mode shape in the load direction (in this example the longitudinal mode shape) is observed. The analysis needs more modes only for the non-linear time integration. Because of this reason just five modes were necessary to compute the Lyapunov exponent from the full system matrices. Fig. 7 shows the obtained mean values and the standard deviations of the Lyapunov exponents.

4.4. Comparison between linear and non-linear analysis

To analyze the quality of the Lyapunov exponents the results obtained from the non-linear column explained in the previous section are compared with the Lyapunov exponents obtained from the linearized system. The linearization was done by using Eq. (42). In Fig. 7 these Lyapunov exponents are compared. The sample analysis of the linearized system uses 100

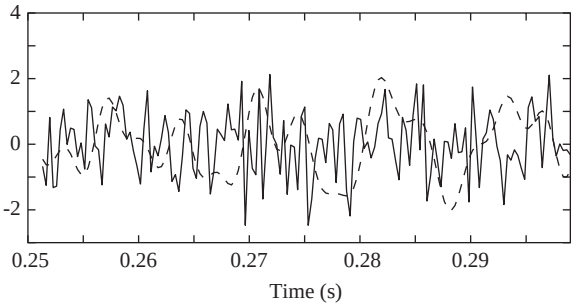

Fig. 8. Comparison of one element of linearized and non-linear stiffness matrices: —, linear; ----, non-linear.

simulations each having 10^5 time steps with $\Delta t = \pi \times 10^{-3}$ s again. The full system is reduced to the size $m = 5$.

The results of both methods show differences at higher load factors. The assumption of similar time fluctuation of the stiffness matrix and the excitation is not exact. This is shown in Fig. 8. Here one element of the tangential stiffness matrix is monitored throughout non-linear dynamic analysis and compared to its linearized counterpart as obtained from Eq. (42). There is quite substantial difference in the time fluctuations.

In this example the linear analysis can be used for a first approximation of the stability boundary. Because of the huge effort of the non-linear analysis, a linear analysis should be applied before the non-linear analysis is used.

4.5. *Effect of prescribed imperfections on non-linear analysis*

The influence of imperfections on the behavior of a non-linear structure was analyzed using the previously described column under random excitation. Imperfections proportional to the first buckling shape were assumed. First investigations of the column discretized with four beam elements led to stabilizing effects with increasing imperfection size which is considered to be infeasible. A static stability analysis of this four element and a 20-element system has shown, that a certain level of discretization is necessary to reproduce the stability behavior correctly. In Fig. 9 the results of these non-linear static calculations are shown. The perfect systems of both variants have nearly the same load dependency. The imperfect four element system does not reach an unstable point, the smallest natural frequency increases above a defined load.

The imperfection influence was investigated for a fixed load factor $\ell = 200$ N on the 20-element model. The magnitudes of mid-span imperfections are varied from 0 to 2.79 cm. The non-linear system was investigated by calculating 20 simulations with 10^5 time steps and $\Delta t = \pi \times 10^{-3}$ s. The destabilizing influence of the geometrical imperfections is easily seen from the results as given in Fig. 10.

4.6. *Reliability analysis of a shell structure*

A cylindrical panel was considered, which is mentioned e.g., in Refs. [3,32,33]. The assumed structure is shown in Fig. 11. The geometrical and the material properties were given as: radius

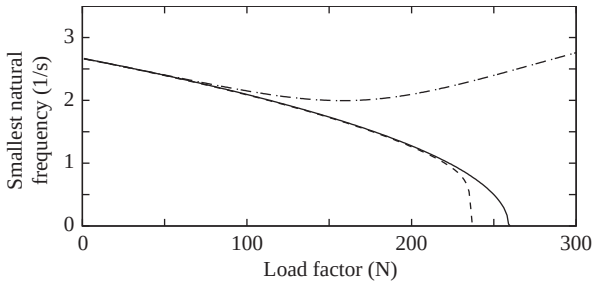

Fig. 9. Static stability behavior using different discretizations: —, perfect system; -·-·-·-, imperfect system, 4 elements; - - - -, imperfect system, 20 elements.

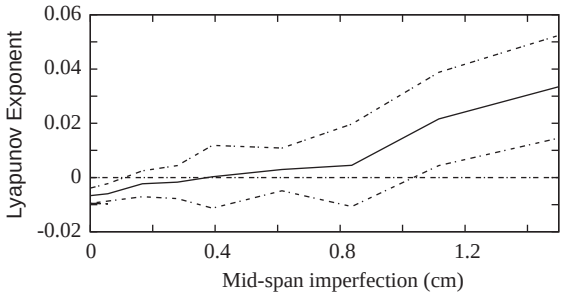

Fig. 10. Top Lyapunov exponent depending on the imperfection size: —, mean value; - - - -, standard deviation.

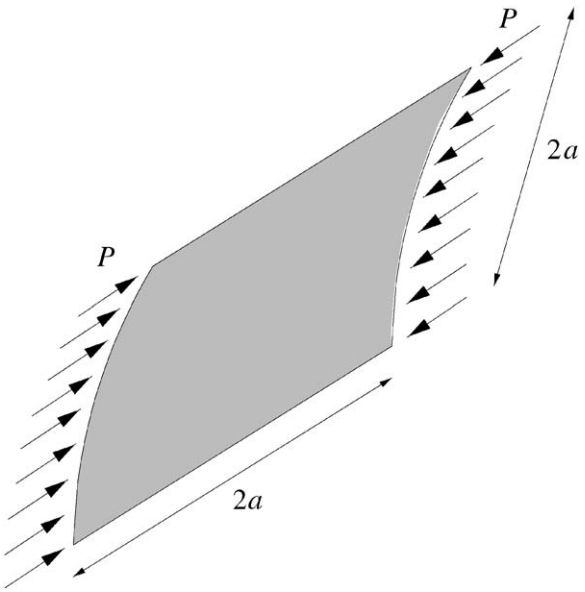

Fig. 11. Cylindrical panel structure.

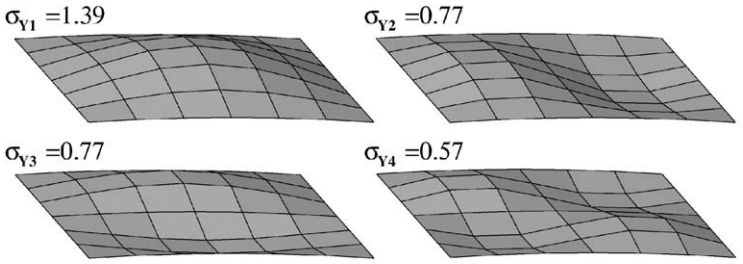

Fig. 12. Weighted imperfection shapes.

$R = 83.33$ m, the half-width and height $a = 5$ m, the thickness $h = 0.1$ m, the Young's modulus $E = 3.410^{10}$ N/m^2, the mass density $\rho = 3400$ kg/m^3 and the Poisson ratio $\mu = 0.2$. The load is assumed according to Eq. (35) as $P(t) = P_0 + P_{\text{fluct}}(t)$. The structure is discretized with 7×7 nodes and meshed with geometrically non-linear 9-node shell elements. At a static load of $P_{0_{\text{crit}}} = 16,825$ kN/m the structure reaches an unstable state [32]: $P_{0_{\text{crit}}} = 15,120$ kN/m, [3]: $P_{0_{\text{crit}}} = 16,200$ kN/m. The static load is assumed to be $P_0 = 0.85 P_{0_{\text{crit}}}$. The fluctuating load is considered as $P_{\text{fluct}}(t) = \ell v(t) \times 1$ kN/m, where $v(t)$ is a unit white-noise process and ℓ is the load factor. The damping is assumed as modal damping with the damping ratios $D_i = 0.02$ for all modes.

The geometrical imperfections are considered in terms of radial deviations from the perfect panel surface. They are modelled as a conditional Gaussian random field as described in Section 3.3. The mean is assumed as zero and the standard deviation as $\sigma = 10^{-3}$ m, which is 1% of the wall thickness. The correlation length of the exponential correlation function is considered with $l_H = 10$ m. The imperfection shapes are obtained by the decomposition of the covariance matrix according to Eq. (39). The first four imperfection shapes are shown in Fig. 12. The corresponding standard deviations σ_{Yj} in uncorrelated normal space are indicated in the figure. The imperfection shape with the largest standard deviation is very similar to the buckling shape.

First the linearized structure was investigated. The first five modes were considered. It was found that only the first imperfection shape has a major influence on the stability behavior.

Then the Lyapunov exponents of the non-linear system are obtained by using 12-mode shapes which requires a maximal time step of $\Delta t = 4 \times 10^{-3}$ s 10^5 time steps and 20 simulations were calculated. The obtained critical noise intensity for the perfect system has the value $D_{0_{\text{crit}}} = 20357\pi$.

To compute the failure probability, it is necessary to interpolate the stability boundaries depending on the imperfection amplitudes. These boundaries are displayed in Fig. 13. It is seen that negative imperfection amplitudes decrease the stability boundary and positive amplitudes stabilize the system. This is caused by the cylindrical shape of the structure. Neglecting the minor influence of the other imperfection shapes the failure probability can by easily calculated under the assumption of normal distribution. The failure probability is shown in Fig. 14 depending on the noise intensity. The figure shows, if the noise intensity reaches the critical value for the perfect system, the failure probability has the size 0.5.

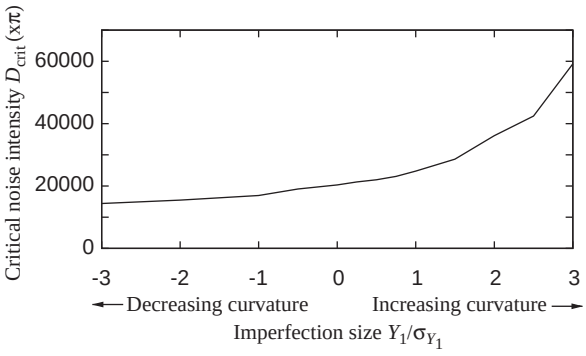

Fig. 13. Stability boundary depending on the imperfection size.

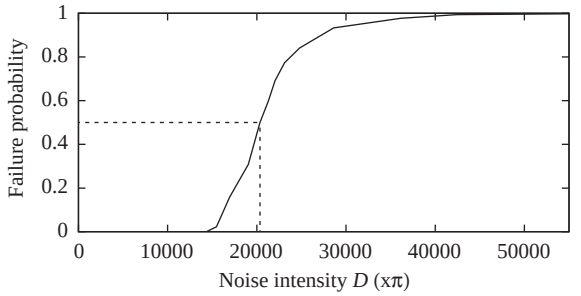

Fig. 14. Failure probability depending on the noise intensity.

5. Concluding remarks

The article presents an approach to consider random geometrical imperfections together with stochastic loading conditions within structural stability analysis. The geometrical uncertainties are modelled by using conditional random fields, the stochastic loading conditions are described in spectral form by using FFT transformation. The geometrical imperfections can be represented as a linear combination of different imperfection shapes with random amplitudes. The loading conditions are assumed to be ergodic. To analyze the non-linear dynamic stability behavior of the system an integration in the time domain is necessary. The used sample time series of the load process are generated by simulation procedures.

The non-linear structural response due to the load processes is computed by explicit time integration schemes. The stability behavior is then computed by using the linearized equation for the neighboring motion around the reference solution. This requires an evaluation of the tangential stiffness matrix at every time step.

This method of non-linear analysis as presented shows several major difficulties. Within a reliability analysis obviously states of the structure which are in the vicinity of the limit state are the most interesting ones. For these cases the integration by an Newmark algorithm may fail, because the stiffness matrix need not necessarily be positive definite any more. To overcome this

difficulty one used a suitably adapted explicit time integration scheme. Since explicit schemes typically require a small time step a projection into a modal subspace is applied to reduce the numerical effort.

Theoretically, the time integration required to estimate the Lyapunov exponents has to be performed until infinity, which of course is not possible. Here a criterion has to be established which is based on the limitation of the variances for the estimator of the Lyapunov exponent, see Eq. (24). Finally and most importantly, in a statistical sense the statement with respect to the Lyapunov exponent, gets less precise as the structural response gets more critical. Thus states which are closer to the limit state require a "longer" loading process and thus a more time consuming integration procedure.

A simplified method based on linear analysis was used to obtain an approximation for the sample stability. This required a linearization of the stiffness matrix with respect to the static loading condition. Of course, this method can be only suitable as long as such a linearization is accurate for the description of the problem. With respect to the numerical effort it seems reasonable that for a stability analysis the linear analysis approach should be applied first to investigate which imperfection shapes are important and at which intensity levels the stability boundaries are reached. In the presented examples it was shown that the influence of non-linearities could be varying significantly for different types of structures. The non-linear analysis method should be applied in each case to validate the obtained stability boundaries or to correct them.

Certainly the number of application for the presented analysis methods is limited "in the real world", as only few structures are submitted to a stationary loading process. Further within a design process a reliability-based stability analysis is of course only one of several required analysis tasks. Especially for the case considered (stationary loading) in this article, fatigue might be at least as relevant for the design process.

Acknowledgements

This research has been supported in part by the German Research Foundation (DFG) under Grant No. Bu 987/3-2, which is gratefully acknowledged by the authors.

References

[1] Y. Schorling, Beitrag zur Stabilitätsuntersuchung von Strukturen mit räumlich korrelierten geometrischen Imperfektionen, Ph.D. Thesis, Bauhaus-University Weimar, Weimar, 1997.

[2] Y. Schorling, C. Bucher, Dynamic stability analysis for structures with geometrical imperfections, in: Naruhito Shiraishi, Masanobu Shinozuka, Y.-K. Wen (Eds.), *Structural Safety and Reliability*, Vol. 2, Balkema, Rotterdam, 1998, pp. 771–777.

[3] Y. Schorling, C. Bucher, Stochastic stability of structures with random imperfections, in: B.F. Spencer Jr., E.A. Johnson (Eds.), *Stochastic Structural Dynamics*, Balkema, Rotterdam, 1999, pp. 343–348.

[4] C. Eller, Lineare und nichtlineare Stabilitätsanalyse periodisch erregter viskoelastischer Strukturen, Technical Report 88-2, Institut für konstruktiven Ingenieurbau, Ruhr-University Bochum, Bochum, 1988.

[5] T.-T. Soong, M. Grigoriu, *Random Vibrations of Mechanical and Structural Systems*, Prentice-Hall, Englewood Cliffs, NJ, 1992.

[6] R. Ghanem, P.D. Spanos, *Stochastic Finite Elements: A Spectral Approach*, Springer, Berlin, 1991.
[7] C.W.S. To, D.M. Li, Largest Lyapunov exponents and bifurcations of stochastic non-linear systems, *Shock and Vibration* 3 (5) (1996) 313–320.
[8] C.W.S. To, M.L. Liu, Lyapunov exponents and information dimensions of multidegree-of-freedom systems under deterministic and stationary random excitations, in: A. Naess, S. Krenk (Eds.), *Advances in Nonlinear Stochastic Mechanics*, Kluwer Academic Publishers, Dordrecht, 1996, pp. 449–458.
[9] A. Wolf, J.B. Swift, H.L. Swiney, J.A. Vassano, Determining Lyapunov exponents from a time series, *Physica* D16 (1985) 285–317.
[10] Y. Schorling, C. Bucher, G. Purkert, Stochastic analysis for randomly imperfect structures, in: R. Melchers, M. Stewart (Eds.), *Applications of Statistics and Probability*, Vol. 2, Balkema, Rotterdam, 2000, pp. 1027–1032.
[11] A. Burmeister, Dynamische Stabilität nach der Methode der Finiten Elemente mit Anwendung auf Kugelschalen, Technical Report No. 6-1987, Institut für Baustatik, University of Stuttgart, Stuttgart, 1987.
[12] W.B. Krätzig, P. Nawrotzki, Computational concepts in structural stability, *Archives of Computational Methods in Engineering* 3 (1) (1996) 81–119.
[13] S.O. Rice, Mathematical analysis of random noise, in: N. Wax (Ed.), *Selected Papers on Noise and Stochastic Processes*, Dover, New York, 1948, reprinted 1954.
[14] C. Bucher, Y. Schorling, W.A. Wall, SLang—the Structural Language, a tool for computational stochastic structural analysis, in: *Proceedings of the Tenth ASCE Eng. Mech. Conference*, *Boulder*, *CO*, May 21–24, 1995, ASCE, 1995, pp. 1123–1126.
[15] C. Bucher, Y. Schorling, SLang—the Structural Language, solving non-linear and stochastic problems in structural mechanics, in: *Proceedings*, *International Conference IKM 1997*, Weimar, Germany, 26.2.-1.3., 1997. Bauhaus-University Weimar, Weimar, 1997.
[16] J.G. Malkin, *Theorie der Stabilität einer Bewegung*, Akademie Verlag, Berlin, 1959.
[17] R. Scheidl, H. Troger, Verzweigungsverhalten eines nichtlinearen Schwingers mit einem doppelten Eigenwert Null, *Zeitschriff für Agewandte Mathematik und Mechanik* 62 (1982) 72–74.
[18] H. Troger, Zum Verfahren von Ritz und Galerkin bei Verzweigungsproblemen, *Zeitschriff für Agewandte Mathematik und Mechanik* 63 (1983) 115–116.
[19] W.B. Krätzig, Y. Basar, P. Nawrotzki, Dynamic structural instabilities, in: W.B. Krätzig, H.-J. Niemann (Eds.), *Dynamics of Civil Engineering Structures*, Balkema, Rotterdam, 1996, pp. 377–449.
[20] P. Boxler, A stochastic version of center manifold theory, *Journal of Probability Theory and Related Fields* 83 (1989) 509–545.
[21] M. Riemer, J. Wauer, W. Wedig, *Mathematischen Methoden der Technischen Mechanik*, Springer, Berlin, 1993.
[22] Y.K. Lin, F. Kozin, Y.K. Wen, F. Casciati, G.I. Schuëller, A. Der Kiureghian, O. Ditlevsen, E.H. Vanmarcke, Methods of stochastic structural dynamics, *Structural Safety* 3 (1986) 167–194.
[23] Y.-K. Lin, G.-Q. Cai, *Probabilistic Structural Dynamics*, McGraw-Hill, New York, 1995.
[24] L. Arnold, P. Imkeller, Fürstenberg-Khasminskii formulas for Lyapunov exponents via anticipative calculus, Technical Report No. 317, Institut für dynamische Systeme, University of Bremen, Bremen, 1994.
[25] K.-J. Bathe, *Finite Element Procedures*, Prentice-Hall, Englewood Cliffs, NJ, 1996.
[26] M. Shinozuka, C.-M. Jan, Digital simulation of random processes and its application, *Journal of Sound and Vibration* 25 (1972) 111–128.
[27] E. Vanmarcke, *Random Fields: Analysis and Synthesis*, MIT Press, Cambridge, 1983.
[28] C.E. Brenner, Ein Beitrag zur Zuverlässigkeitsanalyse von Strukturen unter Berücksichtigung von Systemuntersuchungen mit Hilfe der Methode der Stochastischen Finite Elemente, Ph.D. Thesis, University of Innsbruck, Innsbruck, Austria, 1995.
[29] O. Ditlevsen, Random field interpolation between point by point measures properties, in: *Proceedings of the First International Conference on Computational Stochastic Mechanics*, Corfu, Greece, September 1991, Elsevier, Amsterdam, 1991, pp. 801–812.
[30] C.G. Bucher, Adaptive sampling—an iterative fast Monte Carlo procedure, *Structural Safety* 5 (1988) 119–126.

[31] E. Pardoux, V. Wihstutz, Lyapunov exponent and rotation number of two-dimensional linear stochastic systems with small diffusion, *SIAM Journal of Applied Mathematics* 48 (1988) 442–457.
[32] W.B. Krätzig, Eine einheitliche statische und dynamische Stabilitätstheorie für Pfadverfolgungsalgorithmen in der numerischen Festkörpermechanik, *Zeitschriff für Angewandte Mathematik und Mechanik* 69 (7) (1989) 203–213.
[33] W. Wagner, Zur Behandlung von Stabilitätsproblemen der Elastostatik mit der Methode der Finiten Elemente, Habilitationsschrift, University Hannover, Hannover, 1990.